# BLoB: Beating-based Localization for Single-antenna BLE Devices

Jagdeep Singh[⋆], Michael Baddeley[†], Carlo Alberto Boano[‡], Aleksandar Stanoev[⋆]
Zijian Chai[§], Tim Farnham[⋆], Qing Wang[¶], and Usman Raza[∗]
[⋆]Toshiba Europe Ltd., BRIL, UK; [†]Technology Innovation Institute, AE; [‡]Graz University of Technology, AT;
[∗]Waymap Ltd., UK; [§]University of Bristol, UK; [¶]Delft University of Technology, NL
{jagdeep.singh; aleksander.stanoev; tim.farnham}@toshiba-bril.com, usman.raza@waymapnav.org
michael.baddeley@tii.ae, cboano@tugraz.at, mo20895@alumni.bristol.ac.uk, qing.wang@tudelft.nl

## Abstract

Low-power wireless communication protocols based on *synchronous transmissions* have recently gained popularity. In such protocols, packets can be demodulated correctly even though several devices transmit at the same time, which results in high reliability and energy efficiency. A by-product of synchronous transmissions is the *beating effect*: a sinusoidal pattern of constructive and destructive interference across the received signal. In this paper, we leverage this beating to propose a new localization approach. Specifically, we present BLoB, a system in which multiple anchors transmit packets synchronously using the *constant tone extension*, an optional bit sequence introduced by BLE 5.1, whose signal is sent with constant amplitude and frequency. We let mobile tags sample the superimposed signal resulting from the synchronous transmissions, and extract peaks in the beating and signal spectrum. These peaks provide key insights about the anchors' location that *complement* received signal strength information and allow BLoB to derive a tag's position with *sub-meter* accuracy. A key property of BLoB is that both anchors and tags employ a *single antenna*, in contrast to state-of-the-art localization schemes based on angle of arrival/departure information that require costly and bulky antenna arrays to achieve sub-meter accuracy. We implement BLoB on off-the-shelf BLE devices and evaluate its performance experimentally in both static and mobile settings, and in different environments: office rooms, library, meeting room, and sports hall. Our results show that BLoB can distinguish several anchors in a single synchronous transmission and that it retains a sub-meter localization accuracy even in challenging indoor environments.

*Keywords*

Beating effect, Synchronous transmissions, Constant tone, Bluetooth 5.1, Direction-finding, Signal processing.

## Categories and Subject Descriptors

B.8.2 [**Performance and Reliability**]: Performance Analysis and Design Aids; C.3 [**Special-Purpose and Application-based Systems**]: Real-time and embedded systems, Signal processing systems

## General Terms

Design, Experimentation, Theory, Verification.

## 1 Introduction

Accurate localization of people and objects is a key requirement for several IoT applications, such as asset tracking [1], smart manufacturing [2], and assisted living [3]. Unfortunately, global navigation satellite systems are not applicable indoors due to the inability of satellites' signals to penetrate many structures [4]. To tackle this problem, several works have shown how to leverage ultra-wideband [5], Wi-Fi [6], ZigBee [7], RFID [8], acoustic [9], and optical [10] technologies to develop highly-accurate indoor localization systems. Bluetooth low energy (BLE) is another key technology enabling accurate indoor localization, and is especially attractive due to its *ubiquitous nature* and *low power consumption* [11].

**RSS-based localization is inaccurate.** Many localization systems based on BLE employ single-antenna boards and leverage the *received signal strength* (RSS) of packets to estimate the distance between devices [12, 13, 14], with iBeacon [15] and Eddystone [16] being prominent examples. Unfortunately, RSS-based localization approaches are known to be brittle and have limited accuracy ($\approx$ 1–2.5 meters), as the RSS can easily be affected by changing environmental conditions and human movements, even when carefully calibrating the reference signal strength [17, 18, 19, 20]. Moreover, the performance of RSS-based approaches is strongly affected by the number of employed anchors (the more, the better) and by their careful deployment, which increases costs [21, 22].

**AoA-/AoD-based localization is impractical.** To counter this, BLE 5.1 introduced direction-finding features that support two methods for determining the direction of a signal: angle of arrival (AoA) and of departure (AoD) [23, 24, 25]. These direction-finding features let BLE devices append a *constant tone extension* (CTE) to the transmitted packets, i.e., a sinusoidal waveform with constant amplitude and frequency, as well as continuous phase. A receiver can sample the constant tone and process the in-phase and quadrature-phase (I/Q) components of the received signal, which is

then further processed to perform the AoA/AoD localization [23, 26]. Whilst these techniques allow one to achieve a *sub-meter* localization accuracy by leveraging angular information [27, 28], they require the use of bulky *antenna arrays* (at the receiver for AoA, at the transmitter for AoD). Such antenna arrays are often larger than $15 \times 15$ cm, and hence unpractical for many applications [29]. Moreover, they are costly and hard to find on the market, as the dependence of angular measurements on the antenna separation increases the complexity of the design [30]. AoA/AoD approaches hence face major hurdles w.r.t. wider support and availability.

**Sub-meter localization accuracy with single-antenna?** In this paper, we describe how to retain the simplicity of *single-antenna* RSS-based approaches, while achieving a *sub-meter* localization accuracy that is comparable to that obtained with AoA/AoD-based systems. To this end, we let off-the-shelf single-antenna BLE tags examine the *beating patterns* across a CTE signal received when multiple single-antenna anchors transmit data simultaneously. Recent studies have indeed shown that synchronous transmissions (ST) produce *beating*, i.e., a sinusoidal pattern between two or more signals transmitted at slightly different frequencies, across the received packet [31, 32]. We show that the relative carrier frequency offset (CFO) between devices transmitting simultaneously can be extracted from the received beating pattern, which allows to reliably identify anchors. By exploiting this information and by analyzing the peaks in the beating and signal spectrum, one can identify anchor nodes that strongly contribute to the beating and are hence located nearby the receiving tag. These observations allow to refine the location estimates and to significantly improve the accuracy of an RSS-based localization system running on single-antenna BLE devices.

**Contributions.** Building upon these principles, we design BLoB, a novel BLE-based localization system that can achieve sub-meter accuracy despite the use of small and inexpensive *single-antenna* devices as well as the absence of any angular information. In BLoB, multiple anchors transmit packets synchronously using the CTE, and mobile tags extract the signal characteristics – especially the beating profile – from the superimposed signal resulting from the synchronous transmissions, which enables an accurate position determination.

With BLoB, we make the following contributions:

i) We present signal processing techniques that allow the identification of relevant anchor nodes based on the CFO detected within the beating pattern.
ii) We showcase a method to determine the contribution from a pair of *dominant* anchor nodes within the received beating pattern (i.e., nodes that strongly contribute to the beating and are hence located nearby the receiver), which allows refinement of the location estimate.
iii) We present the design of BLoB, an indoor localization system that integrates the aforementioned solutions and that leverages ST and BLE's CTE feature to achieve accurate localization using *single-antenna* devices only.
iv) We implement a prototypical implementation of BLoB on off-the-shelf Nordic Semiconductor nRF52833 boards with a single PCB antenna. BLoB only requires support for the CTE feature, and it can hence run on any off-the-shelf device compliant to BLE 5.1 and above.
v) We evaluate BLoB's performance experimentally in several indoor environments ranging from large public spaces (e.g., tennis hall) to office rooms. Our results in both static and mobile settings demonstrate that BLoB can retain a sub-meter localization accuracy even in multipath-rich environments. Such performance is superior to classical RSS-based approaches and is comparable to that of AoA-based systems: this is remarkable, given that BLoB runs on *single-antenna* devices and does not make use of any angular information.

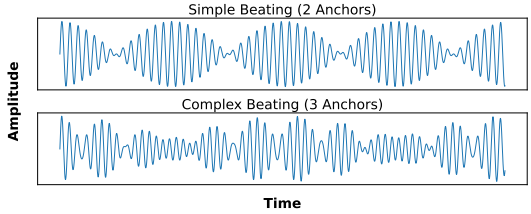

Figure 1: Sinusoidal interference patterns created by *simple* (2 anchors) and *complex* ($>$ 2 anchors) beating [31].

This paper proceeds as follows. After providing background information about ST, beating, and the CTE feature in § 2, we provide an overview of BLoB in § 3, detailing its design and implementation in § 4. We evaluate BLoB's performance experimentally in § 5 and discuss its limitations in § 6. After reviewing related work in § 7, we conclude the paper in § 8.

## 2 Preliminaries

We discuss next how synchronous transmissions lead to the so-called beating effect (§ 2.1) before introducing necessary background information on the BLE 5.1 CTE feature (§ 2.2).

### 2.1 Synchronous Transmissions and Beating

Flooding protocols based on ST have been extremely popular within the low-power wireless community as a means of providing highly reliable multi-hop communications [33]. In contrast to traditional RF communication practices, transmitting nodes in ST-based communications *intentionally* send packets at the same time as their neighbors. While this may seem counter-intuitive (as one would assume the competing signals would collide at the receiver) a high degree of synchronization between nodes and certain physical layer (PHY) aspects of low-power narrowband communications allow successful demodulation of the overlapping signals, specifically *capture effect* and *non-destructive interference* [34].

Particularly in IEEE 802.15.4-based ST and the coded BLE 5 PHYs, the capture effect plays a significant role, allowing successful reception from nodes simultaneously sending *different* data [35]. However, when sending the *same* data (i.e., precisely the same packet or bit sequence, such as a constant tone), successful reception is largely dependent on frequency synchronization between the transmitting nodes [31]. While perfect synchronization would produce constructive interference across the packet and an overall power gain, small manufacturing imperfections result in marginally different carrier frequency offsets. This leads to *non-destructive* interference consisting of sinusoidal periods of *both* constructive and destructive interference across the packet, known

Table 1: Comparison of BLE-based localization techniques.

| Method | Anchor(s) | Tag(s) | Operation |
|---|---|---|---|
| AoA | Single-antenna device transmits packets embedding the CTE | Multiple-antenna device captures the I/Q data of the CTE by switching between antennas | Receiving devices track other objects by measuring the phase difference of the received waveform at different antennas |
| AoD | Multiple-antenna devices transmit a packet embedding the CTE while switching through multiple antennas | Single-antenna device captures the I/Q data of the CTE | Receiving devices track their own positions by measuring the phase difference of the received waveform from different antennas |
| RSS | Single-antenna device transmits packets that do not embed the CTE | Single-antenna device measures signal strength | Receiving devices track their own positions by estimating the distance based on the received signal strength and a reference signal strength |
| **BLoB** | Single-antenna devices synchronously transmit packets embedding the CTE | Single-antenna device captures the I/Q data of the CTE | Receiving devices track their own positions by analyzing the received signal strength at beating and signal frequencies |

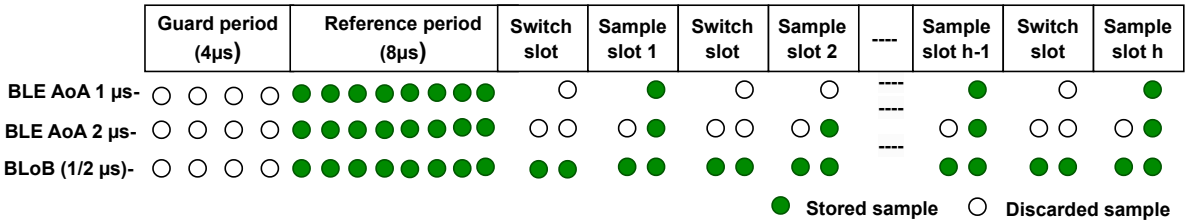


Figure 2: Overview of *CTone* sampling and of the stored I/Q samples at the receiver. Classical systems (e.g., AoA-based [26]) store $h = 74$ or $h = 37$ I/Q samples when using 1 $\mu$s- or 2 $\mu$s-long antenna-switching and sampling slots. In contrast, BLoB uses a *single antenna* and leverages the antenna-switching slot for extra I/Q sampling, which results in up to $h = 148$ collected samples.

as the *beating effect*. Fig. 1 shows an example of *simple* sinusoidal beating pattern created by two synchronous transmitters, and how *complex* beating patterns are created when an additional transmitter is overlapped. Importantly, Baddeley et al. [31] experimentally demonstrated the existence of beating over synchronous transmissions (with an increasing number of nodes) by evaluating errors across a large number of randomly-generated packets, *resulting in clear beating patterns across a histogram of bit errors*. Notably, this study showed that not only is the beating frequency consistent across different PHYs (for the same nodes), but that *different pairs of transmitters produce a frequency that is significantly dissimilar*, due to relative CFO between devices. Moreover, subsequent studies have shown that the relative CFO between synchronously transmitting devices can be predictably modelled and estimated despite temperature variations [36].

## 2.2 Constant Tone Extension in BLE

In BLoB, we leverage the beating signal to capture the relative CFO between devices (anchor nodes) and identify the devices themselves by exploiting the CTE feature in BLE 5.1. The latter allows to append to a BLE packet a constant-frequency signal consisting of unwhitened and constant `1` digits, whose length can vary between 16 $\mu$s and 160 $\mu$s [23]. The purpose of the CTE is to provide a constant wavelength signal (*CTone*) that can be sampled by a receiver, which then processes its I/Q components to derive polar coordinates yielding the phase angle and the amplitude value [25].

The CTE can be divided into several sub-fields, as illustrated in Fig. 2, starting from a guard band of 4 $\mu$s followed by a reference period of 8 $\mu$s. The rest of the CTE field is then divided into slots for antenna switching and sampling. The switching and sampling slots can either be 1 $\mu$s or 2 $\mu$s long: this allows, for example, AoA implementations to choose between a finer localization (faster switching) and a higher energy efficiency, or a simplified antenna design (slower switching) [26]. The CTE field contains $h = 74$ and $h = 37$ samples when using 1 and 2 $\mu$s-long switching and sampling slots, respectively. On the BLE receiver side, while receiving a packet (composed of preamble, access address, protocol data unit, cyclic redundancy check, and CTE), the radio also samples the I/Q components of the baseband signal at 1 $\mu$s frequency. In BLoB, as only single-antenna devices are used, also the I/Q samples in the antenna switching slots can be leveraged, which results in up to $h = 148$ collected samples during the sample slots. The additional number of samples allows the receiver to more effectively separate and decode the individual signals being transmitted and reliably detect beating patterns across all BLE 5 PHY configurations, which makes our approach independent of the underlying PHY. Please note that the CTE field consists of only `1`s with no information attached: there is hence no requirement to demodulate the *CTone* at the receiver.

# 3 BLoB: High-level Overview

We provide a high-level overview of BLoB (§ 3.1), and a detailed description on how ST-induced beating using the *CTone* helps localization of single-antenna BLE mobile tags (§ 3.2).

## 3.1 System Overview

Fig. 3 illustrates BLoB's architecture at-a-glance. In BLoB, spatially-distributed anchors equipped with a *single antenna* synchronously transmit identical packets with empty payload and CTE appended, following a ST-based flooding protocol (detailed in § 4.4). Due to the presence of inherently imperfect crystal oscillators, the *CTone* signals are sent at slightly different frequencies from the intended center frequency by each anchor ($\Delta f_i$). Surrounding tags, also equipped with a single antenna, receive the superimposed *CTone* signal resulting from the synchronous transmissions and perform high-resolution I/Q sampling using up to $h = 148$ samples, as shown in Fig. 2. Signal analysis and beating characterization

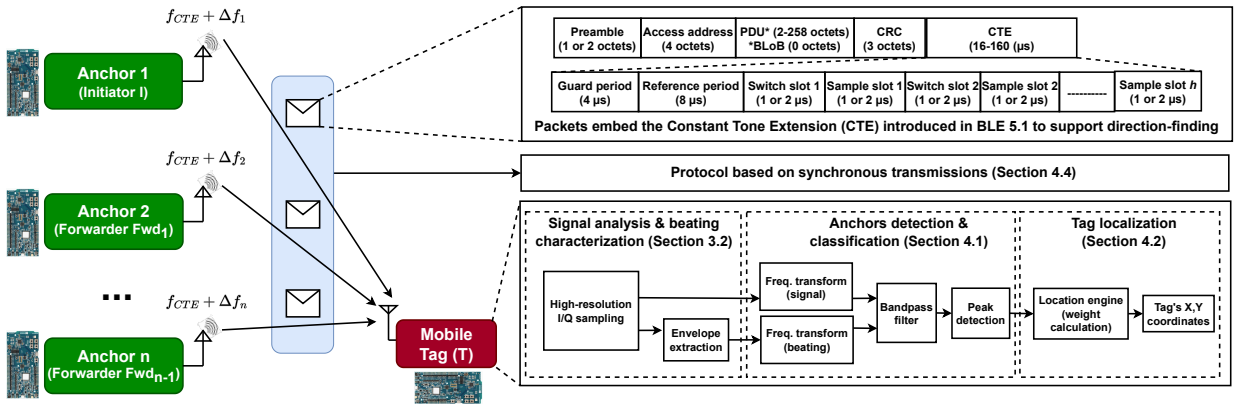


Figure 3: Overview of BLoB, a localization system that uses up to $n$ spatially-separated *single-antenna* anchors synchronously transmitting packets embedding the CTE to localize *single-antenna* mobile tags by examining the beating characteristics across the received signal. One of the anchors acts as initiator (I) and is responsible for time-synchronizing all network operations.

is then performed on the collected I/Q samples (§ 3.2). This serves as input to anchor detection and classification (§ 4.1), and subsequently to tag localization (§ 4.2). Hence, BLoB is fundamentally different from other BLE-based localization approaches, as summarized in Table 1.

## 3.2 Leveraging Beating For Localization

In BLoB, $n$ anchor nodes synchronously transmit sufficiently-long (160 $\mu$s) *CTone* signals with frequencies $(\omega_1, \omega_2, \ldots, \omega_n)$ to produce beating, as shown in Fig. 3. Mathematically, consider the *CTone* signals from $n$ spatially-distributed anchors, represented as:

$$a_1\cos(\omega_1 t), \ldots, a_n\cos(\omega_n t) \text{ and } CTone_i = a_i\cos(2\pi f_i t), \tag{1}$$

where $\omega$ is the angular frequency of the signal in radians and $a_i$ is the amplitude of the $i^{th}$ transmitted signal.

For beating to occur, the *CTone* frequencies $f_1, \ldots, f_n$ should not be equal to each other, and the separation between any two frequencies must not be equal, e.g., the *CTone* frequency can be chosen as:

$$f_i = f_{\text{CTE}} + \Delta f \quad \text{with} \quad \Delta f = (m * f_s)/L, \tag{2}$$

where $f_{\text{CTE}}$ equals to 250 kHz, $\Delta f$ is the frequency offset, $f_s$ is the sampling rate, and $L$ is the length of the *CTone* signal. The parameter $m$ is an integer value, provided $f_i$ should fall in receiver bandwidth. The frequency offset can be deliberately chosen using Eq. 2 to avoid side lobes interference; however, *the inherent CFO caused by the inaccuracy of crystal oscillators is sufficient to analyze beating in BLoB.*

The tag receives the superimposed *CTone* signal (SICT) resulting from the ST. Ignoring any channel impairments for simplicity, such a superimposed signal can be described as:

$$SICT = \sum_{i=1}^{n} A_i\cos(2\pi f_i t), \tag{3}$$

where $A_1, A_2, \ldots, A_n$ are the amplitudes of individual *CTone* signals received at the mobile tag. To obtain the amplitude of the transmitted CTone signal frequencies, the receiver can use the fast Fourier transform (FFT) to analyze the signal spectrum of the received or beating signal. However, the method for extracting the pairwise contribution of the CTone signals in beating will be explained in the following section.

### 3.2.1 Envelope Extraction of the Beating Signal

To extract and analyze the pairwise contributions of anchors' amplitudes in the received beating signal, the tag extracts the *squared* envelop of the received superimposed ST-signal by taking the squared value of the Hilbert transform [37], which can be expressed as

$$\left|\text{Hilbert}\left(\sum_{i=i}^{n} A_i\cos(2\pi f_i t)\right)\right|^2. \tag{4}$$

By applying an FFT on the envelope obtained with Eq. 4, we can characterize the resulting amplitude of beating frequencies and their corresponding power amplitudes, as sketched in Fig. 4. Within the beating spectrum, we can identify a number of peaks, representing the contribution in beating from each pair of anchor nodes. Such contribution is strongly dependent on the tag's position: if the tag is closer to a given anchor, the amplitude of the peaks involving this anchor will be higher: we call such an anchor a *dominant* anchor (or the corresponding beating frequency a *dominant* frequency).

The maximum number of peaks in the beating spectrum is $\binom{n}{2}$. These peaks will be used together with the amplitude of the transmitted *CTone* signal frequencies for localizing a tag's position (see § 3.2.2).

### 3.2.2 High-Resolution Tracking

The frequency power spectrum of the squared envelope of the received analytic signal can be expressed as:

$$\begin{aligned} S_n(\omega) &= 2\pi\sum_{i=1}^{n} a_i^2\delta(\omega) \\ &\quad + 2\pi\sum_{k>l} a_k a_l\left[\delta(\omega-\omega_k+\omega_l)+\delta(\omega-\omega_k-\omega_l)\right]. \end{aligned} \tag{5}$$

where $k$ and $l$ vary between 1 and $n$. $S_n$ is the frequency power spectrum received from the transmitters, whereas $\delta(\omega)$ is a Dirac delta function at the frequency $\omega$.

In BLoB, by examining the peak amplitudes of beating frequencies at $|\omega_k - \omega_l|$ (along with the signal frequencies $\omega_k, \omega_l$ that capture the RSS information from the anchors), one can obtain additional information compared to classical RSS-based localization approaches (which only leverage RSS in-

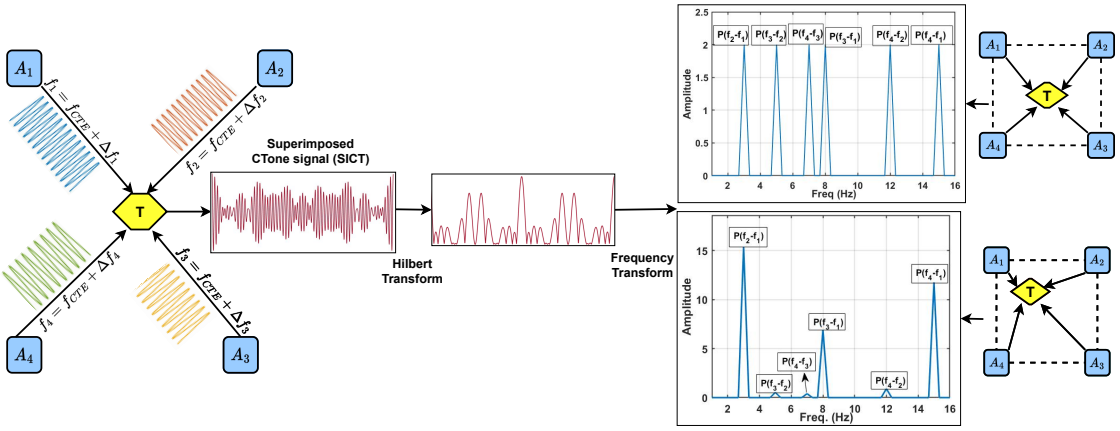


Figure 4: A *single-antenna* tag extracts the squared envelope of the received superimposed signal (i.e., deriving from the *synchronous transmissions* of anchors $A_1, A_2, A_3, A_4$ embedding a *CTone* sent at frequency $f_1, f_2, f_3, f_4$). This allows the tag to determine the contribution of the dominant anchors (by analyzing the highest peaks in the beating spectrum). The top-right figure depicts the case in which there is no dominant frequency in the beating spectrum (in fact, the tag is located at the same distance from all anchors). The bottom-right figure depicts a beating spectrum with a clearly dominant frequency, i.e., that of anchor $A_1$.

formation without beating), and hence increase the accuracy of the localization system. In other words, the computation of the envelope and the extraction of the beating frequencies and amplitudes enables a tag to use additional $N(N-1)/2$ observations (on top of the $N$ observations from the signal spectrum), resulting in a finer location estimate. Notably, the larger number of observations does *not* result in any additional traffic nor higher channel occupancy, and only leads to a negligibly larger expense in terms of signal processing. In § 4.1, we detail how to extract the dominant/true peaks reflecting the signal and beating amplitudes information.

#### 3.2.3 BLoB in Principle

Consider $n = 4$ transmitted *CTone* signals with unit amplitude, represented as $\cos(2\pi f_1 t)$, $\cos(2\pi f_2 t)$, $\cos(2\pi f_3 t)$, $\cos(2\pi f_4 t)$ with *CTone* frequencies $f_1 = 2$, $f_2 = 5$, $f_3 = 10$, $f_4 = 17$ Hz. The tag receives a superimposed signal (Eq. 3) and performs the steps described in § 3.2.1 to extract the amplitude of the signal at the beating frequencies and transmitted *CTone* frequencies. We implement these steps in Matlab assuming a path-loss channel model [38], and derive the illustration shown in Fig. 4.

Specifically, Fig. 4 (top-right) shows the single-sided power spectrum of the squared envelope of the received signal representing the frequency on the x-axis and the received power at those frequencies on the y-axis. A total of six peaks can be identified, i.e., $\binom{n}{2}$, corresponding to the absolute numerical difference between *CTone* frequencies. Moreover, the input CTone signals can be extracted directly from the signal spectrum i.e. by applying an FFT on the received signal.

In this example, we assume uniform power of all transmitted *CTone* signals. For this reason, in Fig. 4 (top-right), where the tag is located exactly at the same distance from all anchors, the peaks corresponding to the six beating frequencies have the same amplitude. A change in the tag's position is reflected as a change in the peak amplitude of the beating frequencies. Fig. 4 (bottom-right) shows an example where the tag moves closer to anchor $A_1$: in this case, the peaks related to $A_1$ are clearly dominant (i.e., their amplitude is higher).

## 4 BLoB: Design & Implementation

We next detail the design and implementation of BLoB with a focus on anchor detection and classification in real-world systems (§ 4.1) as well as on tag localization (§ 4.2). We then model BLoB and analyze its performance in Matlab (§ 4.3). Finally, we present BLoB's ST communication primitive (§ 4.4) used to carry out the evaluation experiments shown in § 5.

### 4.1 Anchor Detection and Classification

The example in § 3.2 assumes a perfect channel model with no impairments. In real environments, due to channel noise and multipath effects, there will be many other peaks in the extracted beating and signal spectrum other than those at the anchor nodes' frequency. Moreover, as BLoB exploits the CFO and does not tune the anchors' clocks, side lobe interference creates more challenges to detect the true peaks in the spectrum. We hence derive a method that allows BLoB to determine the true dominant peaks in the beating and signal spectrum that works in real-world environments.

#### 4.1.1 Peak Searching

To determine the peaks in the beating and signal spectrum (which helps determine the number of anchors present in a ST-based network), BLoB performs the following steps:

(i) Determine all the local maxima values $L_{\max}$ and their neighbor local minima values $L_{\min_1}, L_{\min_2}$ in the received beating and signal spectrum. In the case of the signal spectrum (provided the transmitted *CTone* frequencies are known), the frequency corresponding to local maxima and minima should satisfy the condition:

$$|f_{L_{\max}} - f_{L_{\min_i}}| < \Delta f_{\min} \,, \tag{6}$$

where $f_{L_{\max}}$ and $f_{L_{\min_i}}$ are the signal frequencies corresponding to the local maxima sample point and nearest minima sample point to local maxima, respectively. $\Delta f_{\min}$ is the minimum CFO in the transmitted signal frequencies.

(ii) The local maxima found in step (i) should have amplitudes greater than a threshold $T_1$, which we empirically choose (verified experimentally in § 5) to be equal to $1/5$ of the

maximum received power in the signal spectrum. By setting this threshold, we eliminate the unwanted spectral peaks and channel noise.

#### 4.1.2 Anchor Detection

In BLoB, we exploit *both* the beating *and* the signal spectrum to determine the dominant number of anchors present in the network. We first find peaks in the unfiltered signal and beating spectrum and then configure the cutoff frequency of a fixed impulse response (FIR) filter based on the found peaks. The cutoff frequency for the FIR filter is calculated as follows:

$$f_{\text{lower}} = f_1 * \alpha_1, \quad f_{\text{upper}} = f_2 * \alpha_2, \tag{7}$$

where $f_1, f_2$ are the frequencies corresponding to the first and the last peak found in the spectrum, respectively, whereas $\alpha_1, \alpha_2$ are the redundancy coefficients [39]. Next, we again search the peaks in the filtered spectrum. A decision about the total number of anchors present is made based on the peaks found in the filtered signal spectrum *and* in the beating spectrum. We call this method **`blended approach`** ($M_B$), as it uses *both* beating *and* signal spectrum. For comparison, we also explore an approach that utilizes *only* the signal spectrum, i.e., we only utilize the amplitude at CTone frequency signals, without access to any information about the pairwise amplitude contributions from the beating spectrum (similar to classical RSS methods) to determine the dominant anchors. In this method, which we call **`freq approach`** ($M_F$), the peaks found in the filtered signal spectrum are considered as the number of dominant anchors present.

## 4.2 Tag Localization

In BLoB, we calculate the tag's coordinates based on the amplitude of the received signals at the beating *and* signal frequencies from multiple anchors. Specifically, we use a *weighted centroid approach* to determine the tag position, as in BLoB we have the access to the amplitudes of individual anchor nodes and the contribution of pairs of anchor nodes.

**Step 1 (weights calculation).** We calculate the weights ($W$) corresponding to each dominant synchronous transmitter using the peak amplitude (denoted as $P$) at beating and signal frequencies and assign the weights for the `blended approach`:

$$W(i) = \sum_{i,j=1,i\neq j}^{n} P|\omega_i - \omega_j| + P(\omega_i). \tag{8}$$

**Step 2 (2D localization).** The weighted 2D coordinates $x_r, y_r$ of the mobile tag are computed as:

$$x_r = \frac{\sum_{i=1}^{n}(W(i) * x_t(i))}{\sum_{i=1}^{n} W(i)}, \quad y_r = \frac{\sum_{i=1}^{n}(W(i) * y_t(i))}{\sum_{i=1}^{n} W(i)}, \tag{9}$$

where $x_t(i), y_t(i)$ are the known coordinates of anchor $A_i$.

## 4.3 Preliminary Results from Simulation

To validate the algorithms presented in § 4.1 and 4.2 as well as to further investigate how different profiles of beating and signal frequency amplitude affect the location estimates provided by our approach, we assume a 2D plane of $10\times10\,m^2$ with 4 anchor nodes ($A_1, A_2, A_3, A_4$) at the four corners of the square plane. These anchors operate at 250 kHz, 257.69 kHz, 269.23 kHz, and 273.08 kHz *CTone* frequencies, respectively, which were chosen to satisfy Eq. 2. The length of the CTE packet used is 160 $\mu$s with a sampling rate of 8 Msps. The BLE packets embedding a CTE are generated in a Matlab-based BLE 5.1 simulator [40].

The tag collects the raw I/Q samples of the BLE packet. For further processing of the received signal to obtain the power amplitudes at beating and signal frequencies we evaluate *only* the CTE field in the packet for location estimation, i.e., in BLoB there is no requirement for payload data (§ 4.4). We simulate hundreds of tag locations to determine the position based on our approach, assuming the path loss [38] and Rayleigh fading channel model [41].

Figs. 5a and 5b show the calculated Euclidean localization error (defined as $Er_i(i) = \|l_k - l_{cal}\|$, where $l_k, l_{cal}$ are the known and calculated tag's position, respectively) calculated for the $x, y$ coordinates of the tag at different positions using the `freq approach` and the `blended approach`, respectively. For the `freq approach` (*only* the signal frequency spectrum), we assigned the weight as: $W(i) = P(\omega_i)$.

The cumulative error distribution (CDF) derived over the $Er_i$ of all location estimates for both methods is shown in Fig. 5c under the path loss and Rayleigh fading channel models. Both methods perform well when the tag is located at the centre and receives equal power from all transmitters. However, the `blended approach` performs better when the receiver moves away from the centre position. The calculated mean localization error is 0.6 m and 3.6 m, for the `freq approach`, whereas it is 0.53 m and 2.3 m for the `blended approach`, under the path loss and Rayleigh fading channel models, respectively. This means that the additional information derived by considering the beating characteristics (pairwise contribution of each anchor's power) in the `blended approach` improves the localization performance *by up to 36%* compared to the `freq approach` (which is equivalent to conventional RSS-based localization).

The above results are obtained in simulation. To study BLoB's real-world performance, we implement a ST-based protocol and run it on off-the-shelf BLE devices, as detailed next.

## 4.4 ST-based Communication Primitive

Fig. 6 shows how a ST communication primitive can be modified to support CTE-based analysis of the beating effect. The direction-finding radio extension was used within the ST protocol to generate and receive packets embedding a *CTone*. During the first time slot, forwarders will act as a receiver to perform time synchronization; in the next time slot, they start synchronously transmitting *CTone* signals, and the receiver will perform I/Q sampling. Support was added for the Nordic Semiconductors `nRF52833` SoC [42] to allow the use of the radio's I/Q sampling capability to obtain the raw baseband samples needed for signal beating analysis.

As antenna switching is *not required* in neither transmitters nor receivers, each device role is configured to expect its peer to be responsible for switching. As such, the transmitters are configured for AoA mode, while the receiver is configured for AoD. Other utilized features of the radio peripheral include the ability to capture I/Q samples across the entire received packet, as opposed to just the CTE extension, and the ability to over-sample at a spacing of 125 ns between samples [42]. It should be noted that while the BLoB concept is focused on localization (using an empty payload), there is nothing to pre-

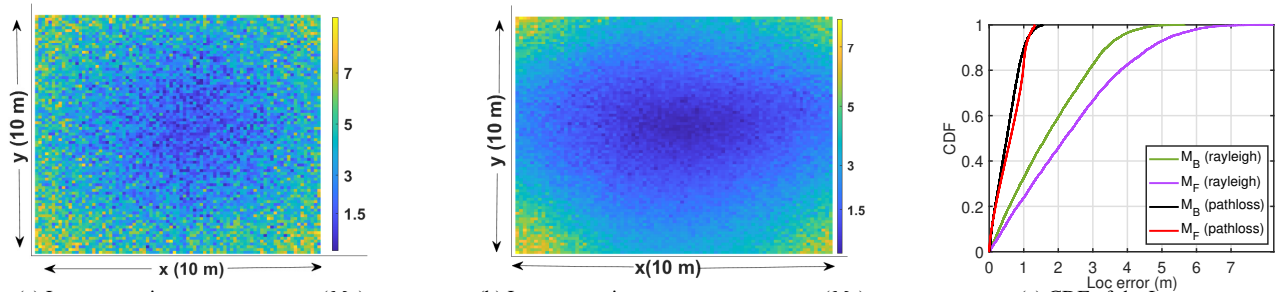


(a) Loc error using `freq approach` ($M_F$) (b) Loc error using `blended approach` ($M_B$) (c) CDF of the Loc error

Figure 5: Analyzing BLoB's localization performance under different channel models in a Matlab environment. The colour bars in Figures 5a and 5b represent the localization error in meters.

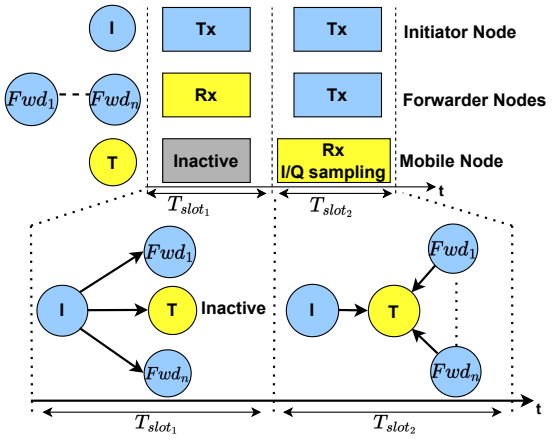


Figure 6: ST-based protocol used in BLoB. The tag (T) syncs on the first timeslot then localizes on the second.

vent BLoB being employed for *simultaneous* communication *and* localization in a ST-based network, provided the protocol ensures that *CTone* from different anchors superimpose. Moreover, with a suitable CTE length, it is possible to detect beating across all BLE 5 PHY configurations – making the approach independent of the physical layer [31].

## 5 Experimental Evaluation

We evaluate the performance of BLoB experimentally. First, we study the accuracy of BLoB in detecting and classifying dominant anchors (§ 5.1). We then quantify BLoB's localization accuracy in various environments and provide a performance comparison with the SOTA AoA technique (§ 5.2).

### 5.1 Detection of Dominant Anchors

We start our evaluation by studying the accuracy of BLoB in detecting and classifying dominant anchors. Our evaluation provides a quantitative answer to the following questions:

- Is the inherent CFO caused by the inaccuracy of crystal oscillators sufficient to discern anchors? (§ 5.1.2)
- Can we detect dominant anchors present in the network by leveraging the beating induced by the CFO? Do packet loss and antenna polarization affect the anchor detection accuracy? (§ 5.1.3)

#### 5.1.1 Experimental Setup

We conduct our experiments using Nordic Semiconductors nRF52833-DK boards in an office room, as shown in Fig. 7,

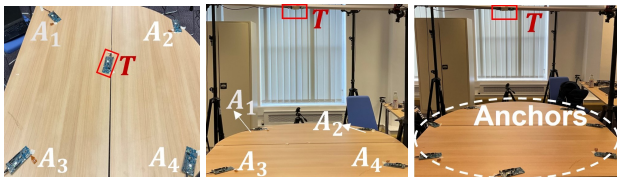


(a) Same plane (b) Different plane (c) Up to 7 anchors

Figure 7: Experimental setup used in § 5.1.

and up to 7 anchors. To test BLoB's anchor detection accuracy, we consider four scenarios:

(S1) Anchors and tag are in the same plane (as in Fig. 7a) with the same antenna polarization;
(S2) Anchors and tag are in the same plane (as in Fig. 7a) with different antenna polarization;
(S3) Anchors and tag are in a different plane (as in Fig. 7b) with the same antenna polarization;
(S4) Anchors and tag are in a different plane (as in Fig. 7b) with different antenna polarization.

#### 5.1.2 Inherent CFO Detection

We start by studying whether the inherent CFO caused by the inaccuracy of crystal oscillators is sufficient to differentiate between anchors in real-world settings. To this end, we measure and compare the *CTone* frequency shift due to CFO for several nRF52833-DK boards. As the latter operate at a carrier frequency of 2.4 GHz, the received baseband *CTone* signal spectrum should peak at $f_{\text{CTE}}$=250 kHz [23]. In practice, this is not the case, as illustrated in Table 2. The CFO varies by as much as 11.69 kHz compared to the nominal *CTone* frequency of 250 kHz. These results confirm that a differentiation of anchors based on their CFO is feasible in real-world settings. The CFO present across different anchors can be determined by following the steps described in the Appendix.

Importantly, while CFO is a property of the radio oscillator and is thus sensitive to environmental factors such as temperature variations, recent work has demonstrated that the relative CFO between synchronously transmitting devices can be predictably modeled and estimated as a function of temperature [36]. This supports the practicality of our approach in harsh environmental conditions.

#### 5.1.3 Anchor Detection

Next, we test BLoB's anchor detection accuracy based on the detection of dominant peaks. We use three configurations:

Table 2: Observed CFO on different nRF52833 boards. Device 685508885 (underlined) acts as initiator. $\Delta f$ represents the detected CFO compared to the nominal 250 kHz value, whilst $\Delta_{init}$ captures the frequency delta w.r.t. the initiator.

| Device ID | Detected *CTone* freq. (kHz) | $\Delta f$ (kHz) | $\Delta_{init}$ (kHz) |
|---|---|---|---|
| 685508885 | 252.453 | +2.453 | 0 |
| 685557904 | 244.756 | -5.244 | -7.697 |
| 685939208 | 250.910 | +0.910 | +1.543 |
| 685695561 | 246.295 | -3.705 | -6.158 |
| 685435368 | 238.600 | -11.40 | -13.853 |
| 685083356 | 261.690 | +11.69 | -9.237 |
| 685465122 | 255.532 | +5.532 | +3.079 |

- *With CRC*: Only the cyclic redundancy check (CRC) passed packets are considered and CRC failed packets are discarded.
- *Without (W/O) CRC*: Only failed CRC packets are used.
- *Both*: Both failed and successful CRC packets are used.

We consider four anchors simultaneously transmitting *CTone* signals (as in Fig. 7a), and tags detecting the presence of dominant peaks in both the beating and signal spectrum. To determine the actual anchors present in the network, we perform the analysis under the *average peak* and *average packet* approach. In the former, the anchor detection accuracy is determined by dividing the total number of true dominant peaks detected in each received packet by the total number of anchors present. In the latter, we first average out the I/Q samples over 20 packets (Empirical Statistical Optimization) and then determine the true dominant peaks. Table 3 summarizes anchor detection accuracy (captured as the number of times in which the number of detected peaks determines the number of actual anchors) obtained over several hundreds runs. It can be seen that the *average packet* approach is more efficient, as the averaging mitigates the impact of channel noise.

**Corrupted packets.** The beating effect may result in packet loss in a communication link [31]. Although, intuitively, this is undesirable, BLoB's performance actually increases when considering the failed CRC packets, as the beating pattern will be more complex – hence leading to a higher detection accuracy, as confirmed from the results in Table 3.

**Antenna polarization.** Further, we analyzed that changing the antenna direction increases the number of CRC failed packets received at the tag (W/O CRC configuration), which in turn creates more complex beating patterns, helps to improve accuracy, as can be analyzed in Table 3. In addition, our results have proved that we can achieve 100% anchor detection accuracy in most cases employing BLoB.

**Maximum number of detectable anchors.** We test the maximum number of nodes detectable with BLoB and the impact brought by the addition of further anchors on the beating signal. We consider the *Both* configuration (i.e., using both failed and successful CRC packets) and analyze it in the S3 scenario. In this configuration, the node detection accuracy was 100% (see Table 3) for both average peak and packet method. To measure the maximum number of anchors that can be detected, we increase the density of anchors in the network by adding a new anchor in each new run in the setup shown in Fig. 7b. Each new anchor is added at an equal distance from the tag. Fig. 7c shows the setup with seven anchor nodes. With the addition of a new anchor in the network, the beating pattern changes (see Fig. 8), affecting the accuracy of anchor detection. In fact, it can be analyzed that, as we increase the number of anchors, more peaks of different amplitude start appearing and the period between valleys decreases in the beating patterns. That is, the peaks start merging in the frequency spectrum, causing the degradation in anchor detection accuracy. Nevertheless, it can be analyzed from Table 4 that BLoB can successfully detect up to 6 anchors with an accuracy of 100% in our experiments.

## 5.2 BLoB's Localization Performance

We continue our evaluation by studying BLoB's localization performance in terms of accuracy, robustness to harsh environments, as well as compare it with the SOTA AoA approach. Our results answer the following questions quantitatively:

- How robust is BLoB localization in dynamic and multipath-rich environments? (§ 5.2.2 and § 5.2.3)
- Does BLoB's performance remain consistent as the testing area increased? (§ 5.2.4)
- How does BLoB perform in mobile settings? (§ 5.2.5)
- Can BLoB achieve a performance that is comparable to AoA-based solutions even though it does not explore phase information? (§ 5.2.6)

### 5.2.1 Experimental Setup

To evaluate the localization performance of BLoB in realistic scenarios, various dynamic multipath-rich environments are being considered, listed in Table 5. These environments include offices, sports halls, libraries, and meeting rooms, each of which contains a variety of reflective and scattering objects such as chairs, desks, monitors, wardrobes, and RF-operated equipment, creating a *multipath-rich* environment. Four anchor nodes are placed in a square formation on tripods at a height of 1.8 $m$ in the offices and sports hall, and on a table at a height of 1 $m$ in the library and meeting room, respectively (see Fig. 10). The tag is placed at randomly-distributed testing positions (denoted as $N_{TL}$) with varying amounts based on the environment being tested (as summarized in Table 5). At least 150 packets are collected at each position and the absolute error at each $N_{TL}$ is calculated as the Euclidean localization error ($E_r$). Results are presented by averaging multiple combinations over time of 10 packets each and computing the CDF over $E_r$. It is important to note that all presented results are raw measurements only, without the use of any filtering techniques such as Kalman or particle filters.

### 5.2.2 Results in Static Multipath-rich Environments

To evaluate the localization performance of BLoB, we first test without the addition of reflective objects in Office 1. The real-time beating and signal spectrum with four active anchor nodes can be seen in Fig. 9a. The results of this localization performance test are presented in Fig. 11a.

**Role of antenna orientation.** We test the robustness of BLoB by evaluating its localization performance with different antenna polarizations in an office environment. As seen in Fig. 11a, the results indicate that the majority of errors (90%) are below 1 m. Furthermore, the mean localization errors for horizontal ($A_h$) and vertical ($A_v$) antenna polarizations

Table 3: Anchor detection accuracy for *avg. peak* and *avg. packet* methods with four anchors with `freq` and `blended` approach.

| Method | Scenario | With CRC (freq) | With CRC (blended) | W/O CRC (freq) | W/O CRC (blended) | Both (freq) | Both (blended) |
|---|---|---|---|---|---|---|---|
| Avg. Peak | S1 | 21.90% | 99.42% | 11.11% | 100 % | 18.65% | 100% |
| | S2 | 19% | 100% | 20.66% | 100 % | 24.45% | 99.18% |
| | S3 | 21.93% | 98.83% | 30.56% | 100 % | 18.21% | 98.55% |
| | S4 | 20.94% | 86.91% | 31.93% | 99.16 % | 12.50% | 89.17% |
| Avg. Packet | S1 | 25% | 100% | 75% | 100 % | 75% | 100% |
| | S2 | 75% | 100% | 100% | 100 % | 75% | 100% |
| | S3 | 100% | 100% | 100% | 100 % | 75% | 100% |
| | S4 | 100% | 100% | 75% | 100 % | 75% | 100% |

Table 4: Anchor detection accuracy using *average peak* and *average packet* methods.

| | | Nodes | | | | | | |
|---|---|---|---|---|---|---|---|---|
| | | 1 | 2 | 3 | 4 | 5 | 6 | 7 |
| Avg. Peak | `Freq` | 100% | 19% | 20.66% | 24.45 % | 3.47% | 1.37% | 0% |
| | `Hybrid` | 100% | 100% | 100% | 99.18 % | 87.28% | 84.96% | 87.96% |
| Avg. Packet | `Freq` | 100% | 100% | 100% | 75 % | 60% | 33.33% | 57.14% |
| | `Hybrid` | 100% | 100% | 100% | 100 % | 100% | 100% | 57.14% |

are 87.55 cm and 107.3 cm, respectively. Whilst in general antenna orientation greatly impacts the localization performance [43], this is not the case in `BLoB`, as it superimposed CTone signals to create beating – less affected by antenna polarization [44].

**Addition of metallic wire.** Further, we externally added a dense/thick metallic wire at the same height of the anchor nodes in Office 1 to test `BLoB`'s performance in more complex reflective environments. Whilst not a full metal sheet, the fence is more than just a simple wire, and adds significant reflections. We tested different placements of metallic wire: one in the x-direction (Fig. 10a) and another in the y-direction (Fig. 10b) w.r.t to setup. Figs. 11b and 11c show that `BLoB` still maintains sub-meter accuracy in a highly-reflective environment. In fact, unlike other BLE localization methods exploiting angular information or RSSI [28], `BLoB` has the capability to handle both low and high reflected environments as it exploits *more sampling points and the beating effect*.

**Performance in the proximity of an anchor.** The simultaneous ranging approaches are susceptible to *dynamic range* problems, as highlighted by [5, 45], particularly when the tag is in close proximity to the anchor node. To test `BLoB`'s performance in such scenarios, we conducted measurements near the anchor $A_4$ ($f_4$) within 1 m radius to the anchor. Although the amplitudes of signals from other anchor nodes transmitting at CTone frequencies $f_1$, $f_2$, and $f_3$ in the signal spectrum are relatively low, the analysis of the beating spectrum (shown in Fig. 9b) helps `BLoB` to determine the pairwise contribution of each anchor's power. As a result, an accuracy of 0.93 m is achieved, which is only 0.07% less than the mean average error obtained in this area.

### 5.2.3 Dynamic Environment

We now evaluate `BLoB` in three more dynamic environments with the placement of anchors at *different heights*: Office 2, a Library, and a Meeting Room (see Fig. 10). The obtained results[1] are presented in Fig. 11d. The Library has more error in localization compared to other environments (93.43 cm), due to multiple book racks, and because the metallic down-ceiling creates more multipath. Nevertheless, the accuracy achieved by `BLoB` is still in the sub-meter range.

### 5.2.4 Large Environment

We also evaluate `BLoB` in a large sports hall with an area of $90m^2$, where it is being tested in one court while the adjacent courts are in use. We use the highly-accurate Optitrack system [46] to provide the ground truth locations of the tag. Specifically, we deployed eight Flex13 motion capture camera systems as shown in Fig. 10f. The Optitrack can be calibrated in a few minutes and provides mm-level accuracy without the need of manually marking fixed positions on the ground. We performed calibration during the first 5 minutes in our experiments and achieved a localization accuracy of 0.401 mm, far less than what BLE can achieve. `BLoB`'s localization accuracy results are presented in Fig. 11e, demonstrating 90% of localization errors achieved are under 1.5 m with a mean average localization error of 116 cm, validating the feasibility of `BLoB` usage for large indoor public spaces.

### 5.2.5 Mobile Scenarios

To validate `BLoB`'s performance in mobile scenarios, we tested with a mobile target in the multipath-rich Office 2 environment during normal office hours (thereby introducing mild RF interference across the 2.4 GHz spectrum in the form of everyday office activities). As shown in Fig. 12, anchors were placed at $A_1$ to $A_4$, creating a 7 m by 1.5 m arena, while the tag was placed on an autonomous robot which moved 6 m along a predefined linear trajectory (this indicates by the red dashed line) from right to left across the middle of the arena. The estimated tag trajectory from `BLoB` is shown in blue, and from 45 samples the mean estimated localization error obtained with the mobile target was 96.58 cm. While this does not represent a full study of `BLoB`'s performance in mobility conditions, this indicated the viability of `BLoB`'s sub-meter localization accuracy in real-world mobile scenarios.

### 5.2.6 `BLoB` vs. AoA-/AoD-based systems

We now show how `BLoB`'s localization performance is comparable to that of AoA-based direction finding solutions, *despite*

[1] All presented results are averaged over different antenna configurations.

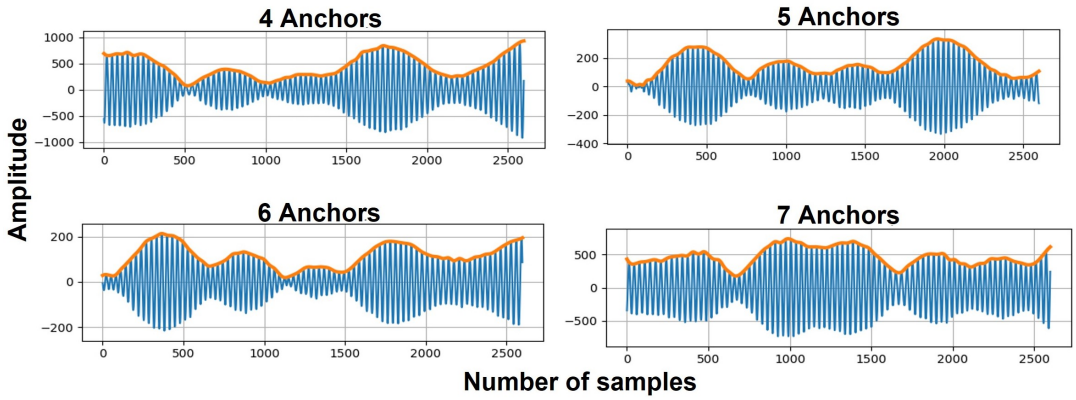


Figure 8: CTE-derived beating patterns at the receiver.

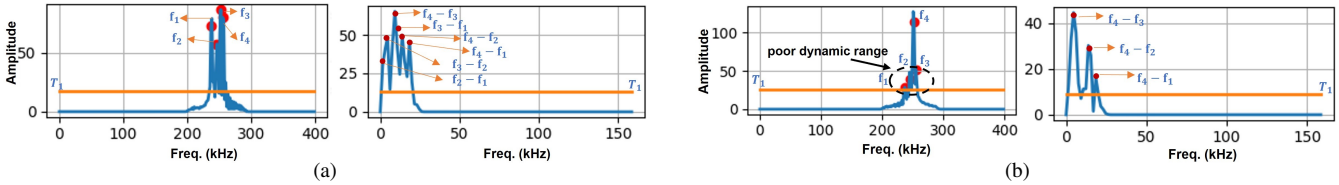


(a) (b)

Figure 9: Office 1: Real-time received signal spectrum (left) as well as received beating spectrum (right) with 4 anchor nodes. Fig. (a) refers to a tag placed in the middle of four anchors; Fig. (b) refers to a tag is in close proximity to anchor $A_4$.

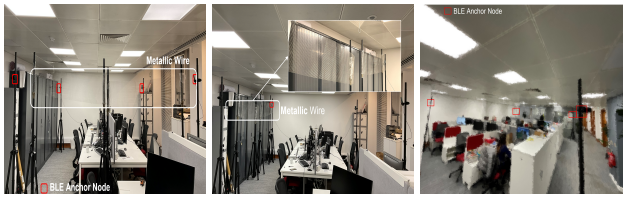

(a) Office 1 (metallic wire in x-direction, $D_x$) (b) Office 1 (metallic wire in y-direction, $D_y$) (c) Office 2

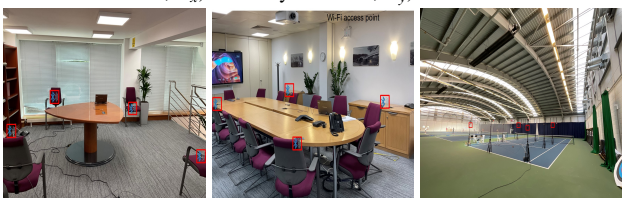

(d) Library (e) Meeting room (f) Sports hall

Figure 10: Environments used in the experiments in § 5.2.

it only uses single antennas and hence does not exploit angular information. When using AoA, a tag is equipped with multiple antennas controlled using an RF switch. By measuring the phase difference observed at the multiple antennas, the tag can locate a transmitter's direction, and perform trilateration to find its position coordinates. If the separation between antennas is known, the AoA is computed using Eq. 10:

$$\theta_A = \arccos((\phi\lambda)/(2\pi D)), \tag{10}$$

where $\lambda$ is the wavelength, $\phi$ is the phase difference, and $D$ is the distance between adjacent antennas in the antenna array. To evaluate the performance of the AoA technique, we employ four multiple-antenna arrays in Office 1 and place the tag at the same locations where we tested BLoB using Silabs EFR32xG22 boards [29] and Silabs' AoA implementation [26, 47, 48]. Fig. 11f shows our results: BLoB achieves a comparable localization performance to that obtained using AoA, also in challenging *non-line-of-sight* (NLOS) conditions (the tag is getting obstructed from two anchors due to the boundary between two tables, see Fig. 10a). Specifically, BLoB exhibits a 50% error of 87.55 cm, whereas AoA-based localization exhibits an error of 95.72 cm. In NLOS conditions, the difference in error is $\approx$ 18.66 cm in favor of BLoB.

## 6 Discussions & Limitations

In this section, we discuss additional features and benefits of BLoB, along with its main limitations.

**Minimizing channel occupancy.** The use of ST reduces the number of transmissions over the air and thus reduces signaling overhead incurred system, *minimizing* channel occupancy. This is a key advantage of BLoB in comparison to classical systems which rely *only* on RSS: the latter require individual responses from each anchor, whereas in BLoB all anchors synchronously transmit a response embedding a CTE. For example, with 4 anchor nodes (A1, A2, A3, A4), in RSS-based localization, multiple transmissions are required between the mobile tag and anchors to record and process RSS values. This process takes at least eight over-the-air transmissions and consumes a significant amount of time. In contrast BLoB, only two over-the-air transmissions over a single channel are needed to complete the process. This considerably reduces the localization time required. The RF footprint in time (channel occupancy) is short to complete such transactions even on the congested Bluetooth advertising channels, the three special ones out of 40 channels.

**Scalable and privacy-preserving localization.** Similar to GNSS-based systems, in BLoB mobile tags are not actively involved in the communication and hence do not disclose their presence. In other words, BLoB enables *fully-passive*

Table 5: Mean BLoB localization error in different scenarios.

| Environment | | Office 1 | | | Office 2 | Library | Meeting Room | Sports Hall |
|---|---|---|---|---|---|---|---|---|
| | | W/o metallic wire | Metallic wire | Blockage | | | | |
| Area ($m^2$), Testing Loc. ($N_{TL}$) | | 20, 52 | 20, 52 | 20, 20 | 15, 15 | 15, 20 | 10, 30 | 90, 30 |
| Mean Loc. Error (cm) | freq | 101.57 | 94.10 | 84.51 | 106.86 | 138.41 | 78.04 | 154.37 |
| | blended | 87.55 | 91.47 | 70.25 | 72.06 | 93.43 | 50.84 | 116.18 |

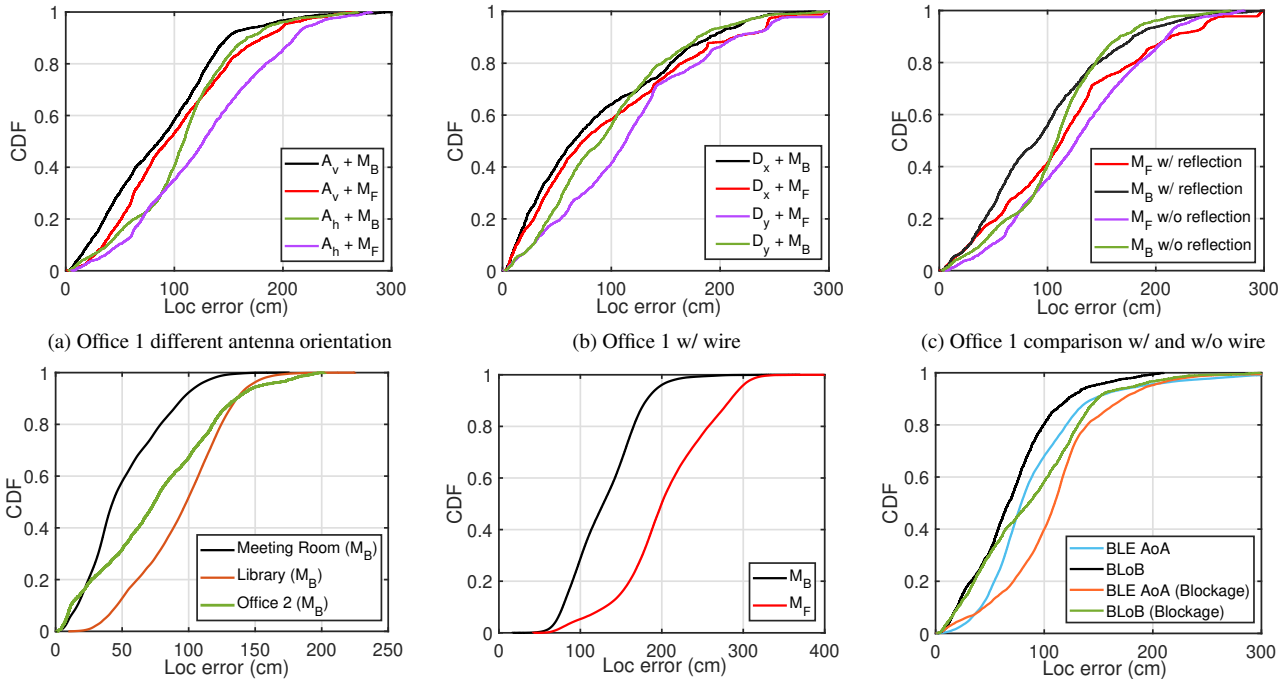


(a) Office 1 different antenna orientation

(b) Office 1 w/ wire

(c) Office 1 comparison w/ and w/o wire

(d) Different indoor environments

(e) Large environment

(f) BLoB vs BLE AoA

Figure 11: CDF of the localization error in different multipath environments. Office 1: different transmitter antenna polarization ($A_v$: vertical, $A_h$: horizontal) w/o metallic wire **(a)**, a metallic wire placed at different positions **(b)**, comparison of Loc. error of setup- with and w/o metallic wire placement **(c)**, Dynamic environment (considering `blended approach`): Library, Office 2, Meeting Room **(d)**, Large indoor tennis hall **(e)**, BLoB's localization performance compared to BLE's AoA technique. The latter uses bulky multiple-antenna arrays and yet achieves a comparable performance to BLoB, which is a single-antenna system **(f)**.

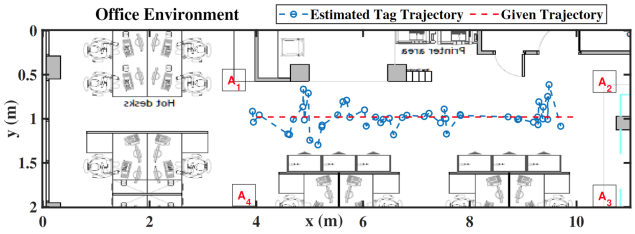


Figure 12: Mobility experiment in the Office 2 environment.

localization that preserves the user's privacy and allows to potentially support countless tags. Moreover, BLoB does not suffer from the disadvantages of AoA/AoD-based systems, where it is challenging to verify the truthfulness of transmitted CTones in such systems, a change in phase introduced by an attacker can cause a significant shift in the AoA [49].

**Channel hopping to improve performance.** In our implementation, we used channel hopping to average out I/Q performance across multiple fading scenarios. As the beating spectrum is dependent on the carrier frequency of all transmitters, averaging out I/Q samples taken across multiple channels increases the probability of sampling a combination that provides large beating amplitudes.

**Computational complexity.** Currently, the signal processing in BLoB is carried out on MATLAB based on the traces obtained with the actual BLE boards. However, the signal processing algorithms employed by BLoB are relatively lightweight, and can be implemented on dual-core BLE-based SoCs such as the nRF5340 by utilizing the second core and the ARM CMSIS-DSP accelerated library to perform the FFT operations required for the algorithm. We will implement such an embedded prototype of BLoB in future work.

**Dynamic range.** The beating amplitudes extracted at the $|\omega_k - \omega_l|$ frequencies can be useful in addressing the dynamic range issue in ST-based localization methods [5, 45]. This issue occurs when the signal strength from one anchor node is much higher than that of other sources, resulting in signal clipping and making it challenging to accurately measure the RSS or the time difference of arrival between the signals. By using beating extraction in BLoB, the pairwise contribution of each anchor's power can be determined, aiding in the calculation of the received power of every anchor node.

## 7 Related Work

**BLE-based localization.** In the pioneer study of BLE 5.1 AoA [49], the authors successfully demonstrated the effectiveness of the technique on USRPs, achieving sub-meter accuracy. However, the testbed scenario was limited to an outdoor environment with few multipath reflections, and the accuracy was calculated by averaging over a large number of packets (1200 phase delay points), resulting in high computational complexity and difficulty in reproducing real-time results. Another experimental demonstration of AoA using SiLabs boards [29, 48] was performed in [27], where the authors reported an average distance error of $0.7m$ using a hybrid solution based on RSS and AoA. However, this study was limited to only *eight* static locations, positions were averaged over 48 packets, and the tests were conducted in a single controlled environment with no consideration for multipath interference. A study by Rinaldi et al. [50] examined the effect of distance on AoA direction-finding techniques for localization in industrial environments. It was found that the angular error increases with distance (even beyond 10 degrees), and that it largely depends on the polarization of the antenna array. Shuai et al. [51] studied the impact of multipath, noise, and antenna switching on AoA calculations, finding an angular error of 12.1 degrees. To mitigate this, two algorithms based on non-linear recursive least square and unscented Kalman filter were proposed, resulting in an improvement of 7.1 degrees for line-of-sight. Finally, it has been observed that direction-finding techniques are highly impacted by channel selection [28, 52]. For instance, [49] studied the impact of channel hopping on AoA and found that the angular error spreads more at lower frequencies. In this context, BLoB, overcomes the current hardware restrictions of AoA/AoD techniques, and has been thoroughly tested in multipath-rich environments with both static and mobile targets, where it sustains sub-meter accuracy.

**UWB-based localization.** Ultra-wideband (UWB) systems are known to achieve a high localization accuracy thanks to their fine-grained timing resolution [5, 53, 54, 55]. UWB radios can in fact process ultra-narrow impulses of 2 ns and precisely estimate the channel impulse response (CIR). By applying signal processing on the CIR, a mobile tag can extract ToA information, which – combined with the known coordinates of the anchors – allows to estimate its position with cm-level accuracy. Unfortunately, narrowband systems such as those based on BLE do not benefit from the fine time resolution and the advanced hardware features present in UWB radios. Nevertheless, BLoB achieves sub-meter localization using BLE, a far more ubiquitous technology than UWB.

**Other wireless localization technologies.** Wi-Fi can provide high-resolution indoor localization systems [6, 56]. However, its high power consumption and the need of special chips for beamforming and time-of-arrival analysis limits its wide adoption [57]. The performance of LoRa for localization is heavily affected by the signal configuration and the environment [58, 59]. Simka et al. [60] reported that the localization error increases by 1.23 m using low-bandwidth signal configurations. Moreover, LoRa's localization performance degrades for short distances and in indoor applications, making it unsuitable for indoor localization at sub-meter accuracy [61].

## 8 Conclusion

In this paper, we have exploited BLE's constant tone extension feature and the beating effect caused by synchronous transmissions to design BLoB, a novel BLE-based localization system capable of localizing mobile tags with sub-meter accuracy despite the use of small and inexpensive *single-antenna* devices as well as the absence of any angular information. We have evaluated BLoB through simulation and real-world experimentation, across various indoor scenarios involving multipath-rich environments, and across both static as well as mobile settings. Our results show that BLoB's performance is superior to classical RSS-based approaches and is comparable to that of AoA-based systems, which, however, rely on bulky, costly, and hard-to-retrieve multi-antenna arrays. BLoB is hence a viable approach for many IoT use-cases in which the use of a bulky multi-array antenna would be impractical.

## 9 Appendix

**Algorithm 1** To examine CFO across anchors in BLoB

**Require:** Extracted Signal & Beating spectrum
**Ensure:** CFO for each anchor

Turn on initiator and find dominant peak $f_1$ using peak search algorithm described in § 4.1.1
**if** Detected peak is not $f_{CTE}$ **then**
    Set CFO as $f_{\text{CTE}} - f_1$
    Set $f_1$ as the true *CTone* frequency
**end if**
**for** each forwarder $Fwd_i$ **do**
    Keep initiator on and activate $Fwd_i$
    Find dominant peaks in the signal spectrum
    **if** two peaks are detected **then**
        Set $f_2$ as the frequency corresponding to the new detected peak
        Set $f_2$ as the *CTone* frequency of $Fwd_i$
    **else if** only one dominant peak is detected **then**
        Observe beating spectrum
        **if** no beating occurs **then**
            $Fwd_i$ shares the same *CTone* frequency with the initiator
        **else**
            Identify dominant beating peak & assign its frequency as $\Delta f_{12}$
            Calculate $f_2$ for $Fwd_i$ as $f_2 = f_1 \pm \Delta f_{12}$ with two values
            Resolve ambiguity by adding a new forwarder and observing the beating spectrum to determine the correct $f_2$
        **end if**
    **end if**
**end for**


## Acknowledgments

We gratefully acknowledge Justin P. Coon (University of Oxford) for his invaluable assistance in the initial verification & validation of the signal-processing techniques. This work has been funded by the European Union's Horizon 2020 research and innovation programme under the Marie Skłodowska Curie grant agreement ENLIGHT'EM No 814215.

# 10 References


[1] F. Ahmed *et al.*, "Comparative Study of Seamless Asset Location and Tracking Technologies," *Procedia Manufacturing*, vol. 51, 2020.

[2] F. Song *et al.*, "Smart Collaborative Automation for Receive Buffer Control in Multipath Industrial Networks," *IEEE TII*, vol. 16, 2020.

[3] K. Witrisal *et al.*, "High-Accuracy Localization for Assisted Living: 5G systems will Turn Multipath Channels from Foe to Friend," *IEEE Signal Process. Mag.*, vol. 33, 2016.

[4] E. D. Kaplan *et al.*, *Understanding GPS/GNSS: Principles and Applications, Third Edition*. Artech House, Inc., 2017.

[5] B. Großwindhager *et al.*, "SnapLoc: An Ultra-Fast UWB-based Indoor Localization System for an Unlimited Number of Tags," in *IPSN*, 2019.

[6] M. Kotaru *et al.*, "SpotFi: Decimeter Level Localization using WiFi," in *Proc. of the ACM SIGCOMM Conf.*, 2015.

[7] D. Lymberopoulos *et al.*, "The Microsoft Indoor Localization Competition: Experiences and Lessons Learned," *IEEE Sig. Proc. Mag.*, vol. 34, 2017.

[8] L. Mo *et al.*, "UHF RFID Indoor Localization Algorithm Based on BP-SVR," *IEEE Journal of Radio Freq. Identification*, vol. 6, 2022.

[9] F. Höflinger *et al.*, "Acoustic Self-calibrating System for Indoor Smartphone Tracking (ASSIST)," in *Proc. of the 2nd IEEE IPIN Conf.*, 2012.

[10] J. Singh *et al.*, "Passive Visible Light Positioning Systems: An Overview," in *Proc. of the LIoT Workshop*, 2020.

[11] T. Savić *et al.*, "Constrained Localization: A Survey," *IEEE Access*, vol. 10, 2022.

[12] Y. Wang *et al.*, "RSSI-Based Bluetooth Indoor Localization," in *Proc. of the 11th MSN Conf.*, 2015.

[13] X.-Y. Lin *et al.*, "A Mobile Indoor Positioning System based on iBeacon Technology," in *Proc. of the 37th IEEE EMBC Conf.*, 2015.

[14] M. Ji *et al.*, "Analysis of Positioning Accuracy Corresponding to the Number of BLE Beacons in Indoor Positioning System," in *Proc. of the 17th IEEE ICACT Conf.*, 2015.

[15] T. Pizer, "White Paper: iBeacon: Matrix Realized," 2015. [Online]. Available: https://bit.ly/3Zfl734

[16] A. Dasgupta *et al.*, "An Internet of Things Platform with Google Eddystone Beacons," *IJSEA*, vol. 9, 2016.

[17] Y. Hu *et al.*, "Experience: Practical Indoor Localization for Malls," in *Proc. of the 28th ACM MobiCom Conf.*, 2022.

[18] J. Powar *et al.*, "Assessing the Impact of Multi-Channel BLE Beacons on Fingerprint-based Positioning," in *Proc. of the 7th IPIN Conf.*, 2017.

[19] L. Yao, "Bluetooth Direction Finding," Ph.D. dissertation, TU Delft, Netherlands, 2018.

[20] J. Kim *et al.*, "Design of MUSIC-based DoA Estimator for Bluetooth Applications," *Journal of IKEEE*, vol. 24, 2020.

[21] Z. Zhu *et al.*, "A Computationally Efficient Method for Direction Finding with Known Transmit Sequence," in *Proc. of IPIN*, 2018.

[22] R. Schmidt, "Multiple Emitter Location and Signal Parameter Estimation," *IEEE Trans. Antennas Propag.*, vol. 34, 1986.

[23] Bluetooth SIG, "Bluetooth Core Specification v5.1," 2019.

[24] Nordic Semiconductor, "Direction Finding nWP-036," 2021. [Online]. Available: https://infocenter.nordicsemi.com/pdf/nwp_036.pdf

[25] M. Woolley, "Bluetooth Direction Finding: A Technical Overview, Version 1.0.3," Oct. 2021.

[26] Silicon Labs, "AN1297: Custom direction-finding solutions using the Silicon Labs Bluetooth stack." [Online]. Available: https://bit.ly/42DCKw9

[27] G. Pau *et al.*, "Bluetooth 5.1: An Analysis of Direction Finding Capability for High-Precision Location Services," *Sensors*, vol. 21, 2021.

[28] M. Qian *et al.*, "Performance Analysis of BLE 5.1 New Feature Angle of Arrival for Relative Positioning," *ISPRS Journal*, vol. 46, 2022.

[29] Silicon Labs, "BG22 Bluetooth Dual Polarized Antenna Array Radio Board." [Online]. Available: https://bit.ly/3ZcB61M

[30] CoreHW, "Antenna Array PCB." [Online]. Available: https://www.corehw.com/products/antenna-array-ant1/

[31] M. Baddeley *et al.*, "The Impact of the PHY on the Performance of Concurrent Transmissions," in *Proc. of the 28th ICNP Conf.*, 2020.

[32] C. Herrmann *et al.*, "RSSISpy: Inspecting Concurrent Transmissions in the Wild," in *Proc. of the 19th EWSN Conf.*, 2022.

[33] M. Zimmerling *et al.*, "Synchronous Transmissions in Low-Power Wireless: A Survey of Communication Protocols and Network Services," *ACM Computing Surveys*, vol. 53, 2020.

[34] A. Escobar, "Improving Reliability and Latency of WSNs using Concurrent Transmissions," *Automatisierungstechnik*, vol. 67, 2019.

[35] R. Jacob *et al.*, "Synchronous Transmissions on Bluetooth 5 and IEEE 802.15.4: A Replication Study," in *CPS-IoTBench*, 2020.

[36] M. Baddeley *et al.*, "Understanding Concurrent Transmissions: The Impact of Carrier Frequency Offset and RF Interference on Physical Layer Performance," *Cornell University – arXiv:2304.00371*, 2023.

[37] M. Johansson, "The Hilbert Transform," Master's thesis, Växjö University, 1999.

[38] D. Grzechca *et al.*, "Analysis of Object Location Accuracy for iBeacon Technology based on the RSSI Path Loss Model and Fingerprint Map," *International Journal of Electronics and Telecommunications*, 2016.

[39] D. Ordóñez-Camacho *et al.*, "An Adaptive-bounds Band-Pass Moving-Average Filter to Increase Precision on Distance Estimation from Bluetooth RSSI," in *Proc. of the 1st ICITS Conf.*, 2018.

[40] MathWorks, "Bluetooth LE Positioning by Using Direction Finding." [Online]. Available: https://bit.ly/40erHrE

[41] Z. Hajiakhondi-Meybodi *et al.*, "Bluetooth Low Energy-based Angle of Arrival Estimation in Presence of Rayleigh Fading," in *Proc. of the 2022 IEEE SMC Conf.*, 2020.

[42] Nordic Semiconductor, *nRF52833 Product Specification*, 2021, v1.5.

[43] J. Xie *et al.*, "Efficient Two-Dimensional Direction Finding Algorithm for Rectilinear Sources Under Unknown Mutual Coupling," *Sensors*, vol. 20, 2020.

[44] M. Baddeley *et al.*, "Atomic-SDN: Is Synchronous Flooding the Solution to software-defined networking in IoT?" *IEEE Access*, vol. 7, 2019.

[45] H. Chen *et al.*, "PnPLoc: UWB Based Plug & Play Indoor Localization," in *Proc. of the 12th IEEE IPIN Conf.*, 2022.

[46] OptiTrack, "OptiTrack - Flex13," [Online] https://optitrack.com/products/flex-13/ – Last accessed: 2023-03-23.

[47] Silicon Labs, "UG514: Using the Bluetooth Direction Finding Tool Suite." [Online]. Available: https://bit.ly/40fECcZ

[48] ——, "QSG175: Silicon Labs Direction Finding Solution Quick-Start Guide."

[49] M. Cominelli *et al.*, "Dead on Arrival: An Empirical Study of The Bluetooth 5.1 Positioning System," in *Proc. of WiNTECH*, 2019.

[50] S. Rinaldi *et al.*, "An Evaluation of Low-Cost Self-Localization Service Exploiting Angle of Arrival for Industrial Cyber-Physical Systems," in *Proc. of the AFRICON Conf.*, 2021.

[51] S. He *et al.*, "Multi-antenna Array-based AoA Estimation Using BLE for Indoor Positioning," in *Proc. of the IEEE ICCC Conf.*, 2021.

[52] H. Ye *et al.*, "A Method of Indoor Positioning by Signal Fitting and PDDA Algorithm using BLE AoA Device," *IEEE Sensors*, 2022.

[53] B. Großwindhager *et al.*, "SALMA: UWB-based Single-Anchor Localization System using Multipath Assistance," in *ACM SenSys*, 2018.

[54] V. Navratil *et al.*, "Concurrent Bi-directional TDoA Positioning in UWB Network with Free-running Clocks," *IEEE Transactions on Aerospace and Electronic Systems*, vol. 58, 2022.

[55] P. Corbalán *et al.*, "Ultra-Wideband Concurrent Ranging," *ACM Trans. Sens. Netw.*, vol. 16, 2020.

[56] X. Chen *et al.*, "Fidora: Robust WiFi-based Indoor Localization via Unsupervised Domain Adaptation," *IEEE IoT Journal*, vol. 9, 2022.

[57] S. Tan *et al.*, "Commodity WiFi Sensing in 10 Years: Status, Challenges, and Opportunities," *IEEE IoT Journal*, 2022.

[58] P. Kanakaraja *et al.*, "LoRA based Indoor Localization using LPWAN Gateway and BLE Beacons," in *Proc. of the IEEE ICEARS Conf.*, 2022.

[59] K. Hu *et al.*, "LTrack: A LoRa-Based Indoor Tracking System for Mobile Robots," *IEEE Tran. on Vehicular Technology*, vol. 71, 2022.

[60] M. Simka *et al.*, "On the RSSI-based Indoor Localization employing LoRa in the 2. 4 GHz ISM Band," *Radioengineering*, vol. 31, 2022.

[61] F. U. Khan *et al.*, "Experimental Testbed Evaluation of Cell Level Indoor Localization Algorithm using Wi-Fi and LoRa Protocols," *Ad Hoc Networks*, vol. 125, 2022.